The Mu2e Solenoid Cold Mass Position Monitor System

T. Strauss, S. Feher, H.W. Friedsam, M.J. Lamm, T. Nicol, T. Page

***Abstract*— The Mu2e experiment at Fermilab is designed to search for charged-lepton flavor violation by looking for muon to electron conversions in the field of the nucleus. The concept of the experiment is to generate a low momentum muon beam, stopping the muons in a target and measuring the momentum of the outgoing electrons. The implementation of this approach utilizes a complex magnetic field composed of graded solenoidal and toroidal fields. Monitoring coil movements of the solenoids during cool down and magnet excitation and cool down is needed. A novel design of a Cold Mass Position Monitor System (CMPS) that will be implemented for the Mu2e experiment has been developed and a prototype CMPS has been built and tested. This paper describes the Mu2e Solenoid System CMPS including the description of the calibration, mounting effort and the CMPS DAQ.**

***Index Terms*—Solenoid System, Superconducting Magnets, Magnetic Field Measurement, Test facilities and instrumentation.**

I. Introduction

The Mu2e experiment [1] at Fermilab is designed to search for charged-lepton flavor violation by searching for neutrinoless muon to electron conversions in the field of a target nucleus. The Mu2e detector consists of three different solenoids [2] to guide muons created in the production target to the muon stopping target and analyze the conversion electrons. Shown in Fig. 1 is the concept of the experiment. A low momentum muon beam is generated using 8 GeV protons delivered from the FNAL accelerator complex that hit a thin tungsten target producing interaction particles inside the Production Solenoid (PS), including pions that will decay into muons. The target is inside a graded magnetic field which will capture some of the muons and subsequently guide them via a Transport Solenoid (TS) to a thin aluminum stopping target inside the Detector Solenoid (DS). Measuring the momentum of the outgoing electrons in a tracker and using a calorimeter for particle identification the muon decays can be further analyzed.

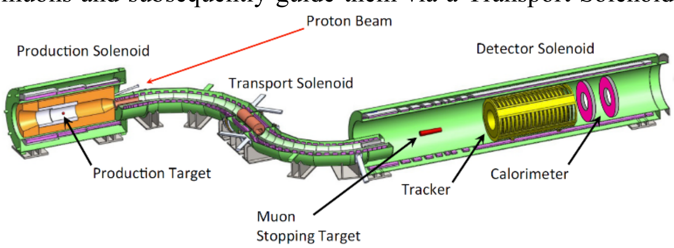

Fig. 1. The Mu2e magnet system [1].

The PS [3] is about 4.5 m long, has a bore of 1.5 m and a gradient field between 2.2 to 4.5 tesla. The PS will be exposed to high radiation levels [4].

The S-shaped TS [5] with a length of about 13.5 m has a field around 2.1 to 2.2 tesla. It contains absorber and collimators. Each of the "L"-shaped arc is made of an independent cryostat; its cold mass is adjustable within ±10 mm [6].

The DS [7], [8] is about 11 m long, with an inner bore diameter of 1.9 m and has a graded field from 1 to 2.1 tesla.

Previous position monitoring system using optical survey [9] or potentiometer [10] did not deliver the required operational range or accuracy. A new approach, translating the cold mass movements into the displacement of a circular planar disk, allows triangulation of said disk at sub-mm accuracy.

This paper describes the CMPS requirements in Section II, the CMPS components in section III, the CMPS calibration and mounting in section IV and the CMPS DAQ in section V.

II. The CMPS Requirements

The DS has the tightest constraints on knowing the magnetic field and solenoid coil positions [11], [12]. As the cryostat houses the muon stopping target, the tracker, and the calorimeter, the field can only be mapped once. Further details on the Mu2e field mapping can be found in [13]-[16]. Mu2e requires to know the position of the DS cold mass with an accuracy of ≤1 mm [17]. The TS and PS position requirements are more relaxed [3], [6], consequently the CMPS accuracy requirements are set to 1 mm.

The solenoid cryostats operate under vacuum (1.3×10^{-9} bar). They are ASME pressure code rated at 1.03 bar (15 psi) in case of cooling pipe ruptures. The CMPS cryostat wall interface must fulfill the same requirements.

The expected peak radiation doses for the PS is 0.3 MGy/year [8], for the TS 10 kGy/year [18] and for the DS 10 Gy/year [19]

We are grateful for the vital contributions of the Fermilab staff and the technical staff of the participating institutions.

This work was supported by the US Department of Energy; the Italian Istituto Nazionale di Fisica Nucleare; the Science and Technology Facilities Council, UK; the Ministry of Education and Science of the Russian Federation; the US National Science Foundation; the Thousand Talents Plan of China; the Helmholtz Association of Germany; and the EU Horizon 2020 Research and Innovation Program under the Marie Sklodowska-Curie Grant Agreement No.690385. Fermilab is operated by Fermi Research Alliance, LLC under Contract No. De-AC02-07CH11359 with the US Department of Energy. The United States Government retains and the publisher, by accepting the article for publication, acknowledges that the United States Government retains a non-exclusive, paid-up, irrevocable, world-wide license to publish or reproduce the published form of this manuscript, or allow others to do so, for United States Government purposes.

T. Strauss is with the Fermi National Accelerator Laboratory, Batavia, IL 60510 USA (e-mail: strauss@fnal.gov). S. Feher, H.W. Friedsam, M.J. Lamm, T. Nicol and T. Page are with the Fermi National Accelerator Laboratory, Batavia, IL 60510 USA.

This manuscript has been authored by Fermi Research Alliance, LLC under Contract No. DE-AC02-07CH11359 with the U.S. Department of Energy, Office of Science, Office of High Energy Physics.

TABLE I
MOVEMENT OF COLD MASSES

Solenoid	Longitudinal movement	Radial movement
TS	15.8 mm to 300 K	3.6 mm to 300 K
PS cool down	20.6 mm to 300 K	<2 mm to 300 K
PS at full current	1.8 mm	-
DS cool down	34.9 mm to 300 K	<5 mm to 300 K
DS at full current	4 mm	-

Movement of the coil components during cooldown, maximal values, see [1] for details. During powering of the solenoid further coil movement is introduced, shown for DS and TS, these movements are much smaller compared to the cooldown.

respectively. The dose value varies several magnitudes along each solenoid position, permanently installed CMPS components must be chosen for peak radiation dose.

The CMPS needs to be able to measure the solenoid coil movements within the abovementioned accuracy for the entire range that is expected during thermal cycles and excitation (powering), summarized in Table I.

The monitoring locations will be exposed to stray magnetic fields, the highest fields are at the PS with ≤0.5 T .

All solenoids will be permanently attached to floor supports after alignment, and entombed behind concrete shielding blocks restricting access. Thus, the CMPS must operate remotely and redundancy must be included in the design.

The solenoids operate at 4.5 K, the wall heat load is intercepted via a thermal shield at 80 K. The most stringent requirement came from the PS, here the additional heat load by the CMPS per solenoid must be less than 1 W.

III. THE COLD MASS POSITIONING MONITOR SYSTEM

In the first approximation, each solenoid is a rigid body, thus one can survey 3 locations to measure its movements. For redundancy, we will have four survey locations on the Detector Solenoid and each arc of the Transport Solenoid. Shown in Fig. 2 is the location of the cold mass position system on one of the Transport Solenoid arcs. For the PS and DS, both have two locations at each end of the solenoids, attached to the cryostat end face.

The system consists of mechanical parts and electronic sensors, shown in Fig. 3. The mechanical part is permanently installed and affixed to the solenoid cold mass and cryostat.

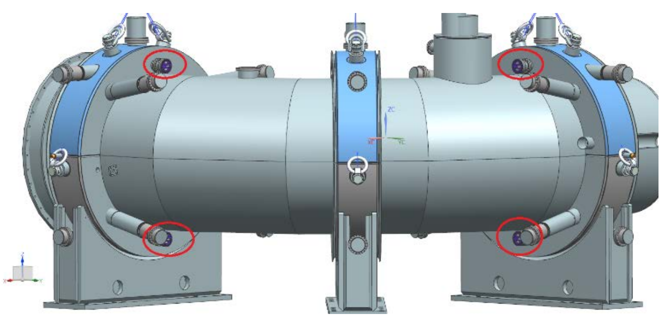

Fig. 2. (Left) The CMPS on the Transport Solenoid assembly. Each of the four locations is marked with a circle.

ConFlat [20] vacuum components with a pressure rated Quartz window seal against vacuum and overpressure.

Made from 6061-aluminum, 316L stainless steel, copper and quartz silica the CMPS is radiation hard at any of the installation locations on PS, TS or DS. The expected dose for each CMPS will be well below the required peak value.

There are few commercially available electronics able to handle the radiation doses of the Mu2e solenoids. As we will utilize the CMPS for PS and TS only for commissioning, we plan to remove the electronics on the PS and upstream TS upon completion of this step. The dose at the DS of about 10 Gy/year enables the operation of some commercial electronics over the three-year duration of the experiment [21]. Should the sensor fail, the mechanical integrity of the CMPS is maintained.

Fig. 3 shows the components of CMPS, with dimensions given in Fig. 4 a). A 3.81 cm (1.5”) sphere rotates freely inside a holder attached to the cold mass, negligible force is needed for movement. A circular planar disk is connected to the sphere by a piston rod; the length of the piston rod differs among the various mounting locations depending on the distances of cold masses relative to the cryostat walls. This circular planar disk slides and tilts within a port tube affixed to the cryostat. The bore of the port tube and the outer edge of the circular planar disk are precision machined to fit. The result of this mounting scheme is a lever arm that follows the cold mass movement via the sphere and converts this movement into a displacement or tilt of the circular planar disk inside the port tube. The component dimensions and tolerances were chosen to assure that one can achieve the desired position resolution and at the same time the disk is able to move freely. A sensor mounting plate allows the trigonometric survey of the circular planar disk at the survey locations shown in Fig. 4b). Three Keyence IL-065 laser sensors [22], with 45 mm range and ±2 µm accuracy, are mounted to the sensor plate. This allows to measure the circular planar disk over the required operational range, summarized in Table 1.

We tested the electronics in fields up to 1 T and found no change in operation.

The CMPS readout works remotely, section V describes the electronic system and redundancy efforts in further detail.

The calculated heat load of the thin rod was estimated to be ≤0.16 W per rod or ≤0.6 W for each solenoid.

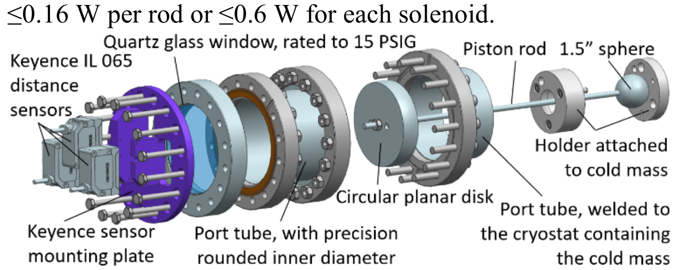

Fig 3. Mechanical Assembly of the Cold Mass Position Monitoring System. Three Keyence IL 065 sensors on a mounting fixture survey a circular planar disk gliding free inside a precision rounded port tube, sealed to vacuum by a fused Quartz Silica window. A piston rod connects the circular planar disk to a 1.5” sphere affixed to the cold mass. Displacements of the sphere with respect to the port tube result in a tilt, roll, yaw or longitudinal displacement of the planar disk. From the three Keyence sensors, the actual displacement can be calculated. The Flange size is a standard ConFlat CF6”, all parts are made from 316L steel, except for the 1.5” sphere and cold mass holder which are constructed from the same 6061-aluminum used for the cold mass.

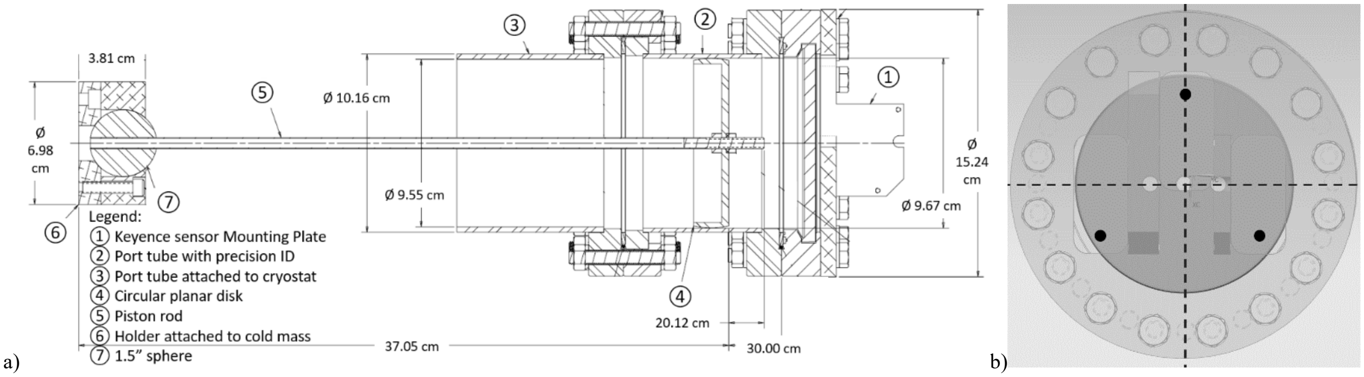

Fig 4. a) Mechanical Drawing of the Cold Mass Position Monitoring System with dimensions in inches. b) The survey locations of the Keyence laser on the circular planar disk, marked with a black circle. View is facing along the piston rod axis of Fig. 4 a).

IV. The CMPS Calibration and Mounting

We measure distances between the mounting plate and disk along the Keyence IL-065 laser paths. Each of the three Keyence IL-065 sensors is attached to a mounting plate without any particular alignment tolerance. Therefore, the three lasers will not be collinear and perpendicular to the mounting plate. This results in small offsets over the measuring range of 50 mm covered by the Keyence IL-065. By calibrating the laser path this can be corrected to achieve higher precision. Each sensor mounting plate has three 0.63 mm (0.25") holes to allow the attachment of 12.7 mm (0.5") spherical reflector nests (.5 SM® (N)-5000-2500-SS) [23]. These three nests build two legs of a local coordinate system while the third dimension is defined by the vector perpendicular to the fitted plane of the outer diameter of the mounting plate, defining the +z-axis pointing towards the spherical moving disk. On an optical table the mounting disk is setup and surveyed, and a movable screen is used to capture the laser spot of the Keyence IL-065 lasers. The beam is mapped at distances of 0, 65 and 2000 mm from the mounting plate. This defines the spatial path of the lasers and the start value of the laser source to better than ± 4 µm absolute per IL-065 (see Fig. 5). The Keyence IL-065 errors result in a miscalculation of the sphere position by ±22.2 µm along the Z vector, and ±74 µm in the transverse directions for the average CMPS piston rod length of 37 cm.

After assembling the mounting plate and window to the port tube, the center axis of the port tube cylinder can be established in the coordinate system of the sensor mounting plate. The orientation of the axis will be known to better than ± 0.5 mrad, resulting in a circular planar disk displacement of up to ±20 µm for the longest movement of the CMPS. The circular planar disk center can travel only along this vector. The three measurements of the IL-065 define three points in the local coordinate system, through which we can fit a plane to the surface of the circular planar disk and infer the location of the cold mass.

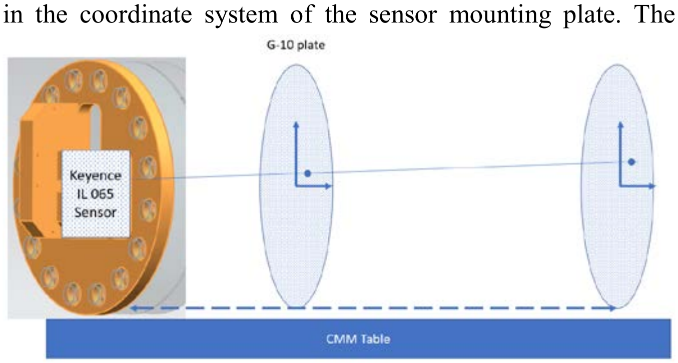

Fig. 5. The calibration idea for the Keyence IL-065 laser path. On a CMM table the sensor plate gets mounted and surveyed. A moveable g-10 screen allows to track the laser path by varying the distance between the sensor mounting plate and the g-10 plate. Optical survey of the laser dot on the plate will establish the laser path in the CMM coordinate system.

Using the normal of the plane, pointing along the same direction as the piston rod, we can calculate the sphere center position for each CMPS location using the correct piston rod length for each device. The piston rod length is adjustable via two setscrews. The effective length of the piston rod needs to be established as follows. First, we measure the center of the spherical mount during the assembly process of the solenoid while it is still accessible. At the same time, we translate this position to a 'secondary' point further away from the cold mass with a detachable fixed-length alignment-rod that can be mounted on the holder with high repeatability using a precision machined shoulder. The sphere and piston rod are then mounted to the cold mass and the solenoid assembly progresses. Via the detachable fixed-length alignment-rod we can re-establish the sphere location at any given time later in the assembly.

Secondly, after the cryostat assembly is completed another survey campaign establishes the cold mass position inside the cryostat using the 'secondary' point, allowing us to calculate the initial sphere position. At this time, the cold mass is no longer visible for direct survey due to the installed heat shield and insulation to reduce the heat load. Now, only the CMPS mounting flange is accessible providing indirect information of the cold mass position. The heat shield has a cutout such that the alignment-rod and piston rod both fit in the same port tube

TABLE II
Error of Estimates of CMPS components

Source	Maximum contribution
Calculated sphere position along the Z vector	±22.2 µm
Calculated sphere position along the transverse directions	±74 µm
Piston Rod: length error, metrological survey	±25 µm
Port Tube: Angular tilt	±20 µm
Squared root of the sum of the squared errors	±83.6 µm

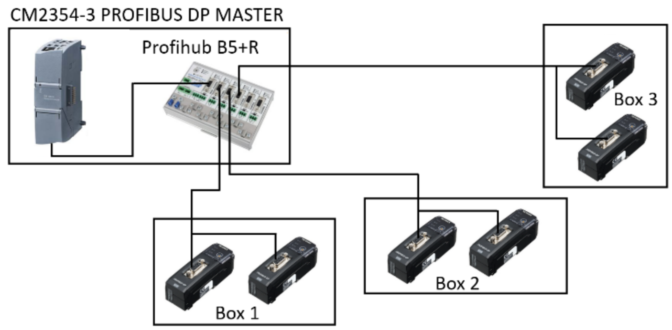

Fig. 6. The PROFIBUS architecture of the CMPS the three instrumented solenoids (2 arcs of the transport Solenoid and Detector Solenoid).

opening. Using a small support jig the piston rod length is adjusted so the circular planar disk will be within the measurement range of the three IL-065 sensors for the predicted cold mass movements after the CMPS is mounted to the port tube. The thickness of the precision machined circular planar disk can be measured in the jig by following the outer edges of the planar disk. This establishes the center of the planar disk for the tilt and displacement of the piston rod and sphere assembly. The distance between this center and the sphere location defines the piston rod length; the surveyed length should be known to better than ±25 µm.

We expect the errors to be independent. Summarized in Table II, the estimated error between the cold mass position and CMPS reading is less than ±100 µm, well below the design requirement of ±1 mm. We measured the difference between the sensor reading and metrological survey with a prototype and found a discrepancy of about 300 µm for the longest travels. This unexpected error contribution came from the imperfect flatness between piston rod and circular planar disk in the prototype. Yet, the measurements showed a repeatability of better than 20 µm.

V. The Data Acquisition System

The readout of the CMPS must be remote controlled. During operation, the system records position data every few minutes. The crucial requirement is repeatability and accuracy. The Keyence IL series [22] uses rack mountable amplifier modules. As each solenoid has 12 IL-065 sensor heads, we use two IL-1000 master amplifiers with five IL-1050 slaves each per solenoid. Each IL-1000 amplifier is connected to a Keyence DL-PD1 PROFIBUS communication unit [24]. For redundancy two 24 V DC power supplies are used. The Keyence IL-065 sensor is set to read at the one µm level with a 4 s sampling time for the highest accuracy. These items are assembled in an electrical enclosure that is placed inside the concrete shielding, with a 110 V AC service-line and the PROFIBUS cable routed outside. Redundant 24 V power supplies are installed.

Fig. 7. The full assembly of the CMPS readout for the Detector Solenoid. Shown are the two Keyence DL-PD1 units with the six amplifiers for the IL-065 sensor heads (one Keyence IL-1000 master and five Keyence IL-1050 slaves). Redundant power supplies increase the operational functionality. A SIEMENS S7-1200 PLC with a CM2354-3 PROFIBUS master extension allows to read the sensor head data and compute the displacement.

The DAQ is based on programmable logic controller (PLC, [25]) infrastructure to comply with the Mu2e cryogenic slow control system; 'Structured Text' [26] program language is used to calculate the position of the sphere. Shown in Fig. 6 is the PROFIBUS network connecting the slow control PLC with each of the three CMPS readout boxes, a star architecture using a Procentec PROFIBUS B5+R hub [27] is chosen to prevent single point failure of the communication service.

To use the CMPS at the PS and DS manufacturing site, a SIEMENS S7-1200 PLC [28] was added to one electric box, shown in Fig. 7. This will allow to calculate the cold mass movement in-situ. Before the installation at the Mu2e detector hall this PLC will be removed. As mentioned before, the radiation dose near the Production Solenoid will likely damage the Keyence IL-065 sensor heads on the TS, thus the upstream sensors will be removed as monitoring is not needed after the initial alignment, only the two most downstream sensors remain to help understand the DS-TS interface changes over time.

VI. Conclusion

We have presented the design of the Mu2e Cold Mass Position Monitoring System designed to remotely operate over the three-year lifetime of the Mu2e experiment. The mechanical components are designed to survive the radiation, vacuum and pressure requirements. Estimation of the error indicates an achievable resolution of better than ±100 µm. The system was tested with optical survey equipment and better than ±300 µm position accuracy was achieved, with repeatability of better than 20 µm, limited by the manufacturing process of the prototype.

References

[1] Mu2e Collaboration (L. Bartoszek et al.), "Mu2e Technical Design Report", FERMILAB-TM-2594, FERMILAB-DESIGN-2014-01, Oct 2014, e-Print: arXiv:1501.05241

[2] M. J. Lamm, et al., "Solenoid Magnet System for the Fermilab Mu2e Experiment", *IEEE Trans. Appl. Supercond*., vol. 22, no. 3, 2012, Art. no. 4100304.

[3] V. V. Kashikhin, et al., "Conceptual Design of the Mu2e Production Solenoid," *IEEE Trans. Appl. Supercond*., vol. 23, no. 3, 2013, Art. no. 4100604.

[4] V. V. Kashikhin, et al., "Reference Design for the Mu2e Production Solenoid," Mu2e-doc-3647 (2013).

[5] G. Ambrosio, et al., "Challenges and Design of the Transport Solenoid for the Mu2e Experiment at Fermilab", *IEEE Trans. Appl. Supercond*., vol. 24, no. 3, 2014, Art. no. 4101405.

[6] M. Lopez, et al., "Mu2e Transport Solenoid Cold-Mass Alignment Issues", *IEEE Trans. Appl. Supercond*., vol. 27, no. 4, 2017, Art. no. 4500405.

[7] S. Feher, et al., "Detector Solenoid Reference Design Report", Mu2e-doc-3664 (2013).

[8] S. Feher, et al., “Reference Design of the Mu2e Detector Solenoid”, *IEEE Trans. Appl. Supercond*., vol. 24, no. 3, 2014, Art. no. 4500304.
[9] D. Goldstein, D. Saltzberg, “The RASNIK real-time relative alignment monitor for the CDF inner tracking detectors”, *Nucl. Instrum. Meth. A*, vol. 506, no. 1-2, 2003, page 92-100
[10] R.J.M.Y. Ruber, et al., “ATLAS superconducting solenoid on-surface test”, *IEEE Trans. Appl. Supercond*., vol. 15, no. 2, 2005, pp. 1283.
[11] R. Ostojic, et al., “Challenges in the Design of the Detector Solenoid for the Mu2e Experiment”, *IEEE Trans. Appl. Supercond*., vol. 23, no. 3, 2013, Art. no. 4500404.
[12] M. J. Lopez, et al., “Studies on the Magnetic Center of the Mu2e Solenoid System”, *IEEE Trans. Appl. Supercond*., vol. 24, no. 3. 2014, Art. no. 4100604.
[13] M. Buehler, S. Gluchko, M. L. Lopes, C. Orozco, M. Tartaglia, J. Tompkins, “Mu2e Magnetic Measurement Studies”, *IEEE Trans. Appl. Supercond.*, vol. 24, no. 3, 2014, Art. no. 9001004.
[14] M. Buehler, M. Tartaglia, J. Tompkins, C. Orozco, “Mu2e Magnetic Measurements”, *FERMILAB-CONF-13-268-TD*, Proceedings, 5th International Particle Accelerator Conference (IPAC 2014): Dresden, Germany.
[15] C. Orozco, et al., “Hall Probe Calibration System Design for the Mu2e Solenoid Field Mapping System”, *IEEE Trans. Appl. Supercond*., submitted for publication.
[16] S. Feher, et al., “The Mu2e Solenoid Field Mapping Design”, *IEEE Trans. Appl. Supercond*., submitted for publication.
[17] M. J. Lopez, “Tolerance Studies of the Mu2e Solenoid System”, *IEEE Trans. Appl. Supercond*., vol. 24, no. 3, 2014, Art. no. 3800105.
[18] V. S. Pronskikh, “Radiation Studies for the Mu2e experiment: A Review”, *Mod. Phys. Lett. A*, 28, 1330014 (2013).
[19] V. S. Pronskikh, “Dose levels at the critical locations of the TS and DS”, Mu2e-doc-3593 (2013).
[20] Kurt J. Lesker Company, “CF Flanges Technical Notes”, http://www.lesker.com/newweb/flanges/flanges_technicalnotes_conflat_1.cfm?pgid=0.
[21] Keyence Cooperation, “CMOS Multi-Function Analog Laser Sensor, IL Series”, https://www.keyence.com/products/measure/laser-1d/il/index.jsp.
[22] NASA, “TOTAL DOSE CHARACTERIZATION TESTS”, https://radhome.gsfc.nasa.gov/radhome/papers/TIDPart.html.
[23] Hubbs Machine & Manufacturing Inc, “Holder for .5000 Spherically Mounted Retro-Reflector .5 SM® (N)-5000-2500-SS”, https://hubbsmachine.com/laser-tracker-5-sphere-mount-/127-5-sm.html.
[24] PROFIBUS (Process Field Bus), standard for fieldbus communication in automation technology, http://www.profibus.com.
[25] Programmable logic controller (PLC), https://en.wikipedia.org/wiki/Programmable_logic_controller.
[26] Structured Text, https://en.wikipedia.org/wiki/Structured_text.
[27] Procentec, ProfiHub B5+R for creating star networks, https://procentec.com/products/profihub/units/profihub-b5plusr/
[28] SIEMENS, “SIMATIC S7-1200 - SIMATIC Controllers”, https://www.siemens.com/global/en/home/products/automation/systems/industrial/plc/s7-1200.html.